

Multiphoton ionization of Mg in the wavelength region of 300–214 nm

Y. L. Shao, C. Fotakis, and D. Charalambidis

*Foundation for Research and Technology-Hellas, Institute of Electronic Structure and Laser,
and Physics Department, University of Crete, P.O. Box 1527, 71110 Heraklion, Crete, Greece*

(Received 11 May 1993)

The results of an experimental spectroscopic study of the $3pn p\ ^1S^e$ ($n=3-6$) and $3p4f\ ^1D^e$ autoionizing states of Mg populated via two-photon absorption are presented and compared with those of different recent theoretical calculations. The study includes excitation spectra and electron angular distributions resulting from the autoionization decay. Photoelectron angular distributions following resonantly enhanced multiphoton ionization via the $3s3p\ ^1P$, $3s4s\ ^1S$, and $3s3d\ ^1D$ intermediate states are also reported and discussed. A strong observed single-photon excitation of the $3s3d\ ^1D$ state via an electric quadrupole transition is also presented.

PACS number(s): 32.80.Dz, 32.80.Rm, 32.80.Fb

INTRODUCTION

Multiphoton ionization has proved to be a useful technique for studies of atomic structure, especially for states of such parity or angular momentum that they cannot be excited from the ground state via one-photon absorption. This is the case for the even-parity states of the alkaline-earth atoms. From these states, of particular interest are a series of doubly excited states, which lie energetically above the ionization threshold and thus autoionize via Coulombic interaction of the two excited electrons. Such highly excited states are suitable for studies of the electron-electron rest interaction and the resulting configuration mixing since the two excited electrons are strongly correlated, a special case of the highest degree of correlation being provided by configurations of the type nl^2 . Furthermore, another important aspect of such doubly excited states is their relevance to the problem of non-resonant double or multiple ionization of atoms in a strong laser field [1]. Additionally autoionizing states are favorable candidates for amplification or lasing-without-population-inversion [2] schemes, as well as in providing enhanced selectivity for laser isotopic separation.

Several studies on doubly excited series of alkaline-earth elements have been performed experimentally as well as theoretically [3]. Although the lighter elements can be considered less complicated for theoretical calculations and their spectra to show reduced complexity, only the heavier elements such as Sr and Ba have been extensively studied experimentally. Few measurements exist for Ca [4]. Among the alkaline-earth elements, Mg has only recently been investigated experimentally. The reason for this is that its high ionization potential and the lacking of a $(n-1)d$ -subcell configuration (n being the principal quantum number of the ground state) require rather short wavelengths in order to excite its autoionizing states. Thus apart from the measurement of Bonanno, Clark, and Lucatorto [5] for the $3p^2\ ^1S$ state, only some odd-parity autoionizing series have been recently reported [6].

In the present work, we report the observation of

even-parity autoionizing states of Mg in two-photon ionization spectra in the wavelength region 300–214 nm. The spectra are discussed and compared with those of the calculations of Chang and Tang [7,8] and Moccia and Spizzo [9]. One of the observed peaks in the resonantly enhanced ionization spectra is shown to originate from the single-photon quadrupole excitation of the $3s3d\ ^1D$ state. In addition, angular distributions of electrons produced by the decay of autoionizing states and through several resonantly enhanced multiphoton ionization schemes are presented, discussed, and compared with the available theoretical angular distribution work of Tang [8].

EXPERIMENTAL SETUP

The experimental apparatus is comprised of three components: the laser system, the vacuum chamber containing an electron-energy analyzer connected to the Mg atomizing oven, and the data-acquisition system. A schematic diagram of the system is shown in Fig. 1.

The laser system consisted of a XeCl excimer (Lambda Physik LPX315) pumped dye laser (Lambda Physik FL3002) having a bandwidth of $\sim 0.2\text{ cm}^{-1}$ and a pulse duration of $\sim 13\text{ ns}$. The second harmonic (SH) of the

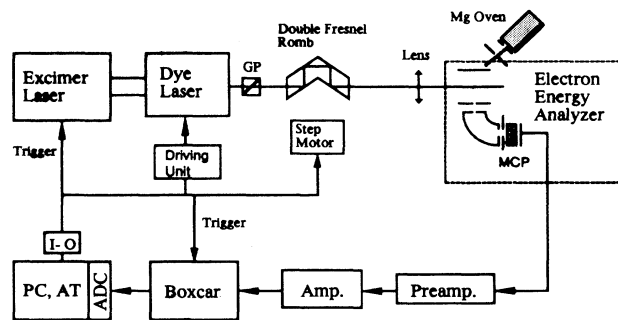


FIG. 1. A schematic diagram of the experimental setup. (See text for a detailed description.)

output of several dyes has been used in order to cover the spectral region of interest, 300–214 nm. A Glan prism polarizer was inserted between the preamplifier and the main amplifier of the dye laser in order to purify the polarization and diminish the amplified spontaneous-emission background. The SH was generated in different barium borate (BBO) crystals according to the wavelength region and was separated via a four Pellin-Broca prism separator. The overall SH output was $\sim 1\text{--}5$ mJ. The SH radiation was intersecting the Mg atomic beam at right angles either unfocused or focused with an $f = 15$ or 30 cm lens, so that the power density at the interaction area could be varied between ~ 1 MW/cm² and 1 GW/cm². A double Fresnel rhomb (B. Halle) and a Soleil-Babinet retarder (Stieg & Reuter) have been used for the rotation of the plane of polarization of the beam and for changing its polarization from linear to circular, respectively.

The effusive magnesium atomic beam was produced by a resistor-heated oven, isolated from the main chamber with a water-cooled baffle, and maintained at a temperature of 410°C corresponding to a Mg vapor pressure of $\sim 5 \times 10^{-3}$ mbar. The Mg atoms entered the vacuum chamber, pumped down with a turbo molecular pump to a background vacuum less than 10^{-6} mbar, through a 1-mm-diam aperture. The atomic beam was collimated

through a guiding tube having its aperture in front of the interaction area.

A 120° spherical-sector electrostatic energy analyzer (COMSTOCK) placed in the vacuum chamber was used for the detection of the ionization products. By applying appropriate voltage polarities, the analyzer could be operated either as an ion “time-of-flight” mass spectrometer for the recording of the ionization spectra, or as an electron spectrometer for the measurement of the photoelectron energy and angular-distribution spectra.

The signal of the analyzer was amplified via a preamplifier (CANBERRA 2005) and main amplifier (CANBERRA 2013), integrated in a boxcar integrator (EG&G), the output of which was digitized and stored in a personal computer, which was also controlling the experimental runs.

RESULTS AND DISCUSSION

Excitation spectra

The two-photon ionization spectra of Mg in the excitation wavelength region 300–214 nm are depicted in Figs. 2(a)–2(d). The absolute wavelength calibration with an accuracy of 2 cm^{-1} is based on the energies of the $3p\ ^1P$, $3d\ ^1D$, and $4s\ ^1S$ states taken from the Mg energy level of

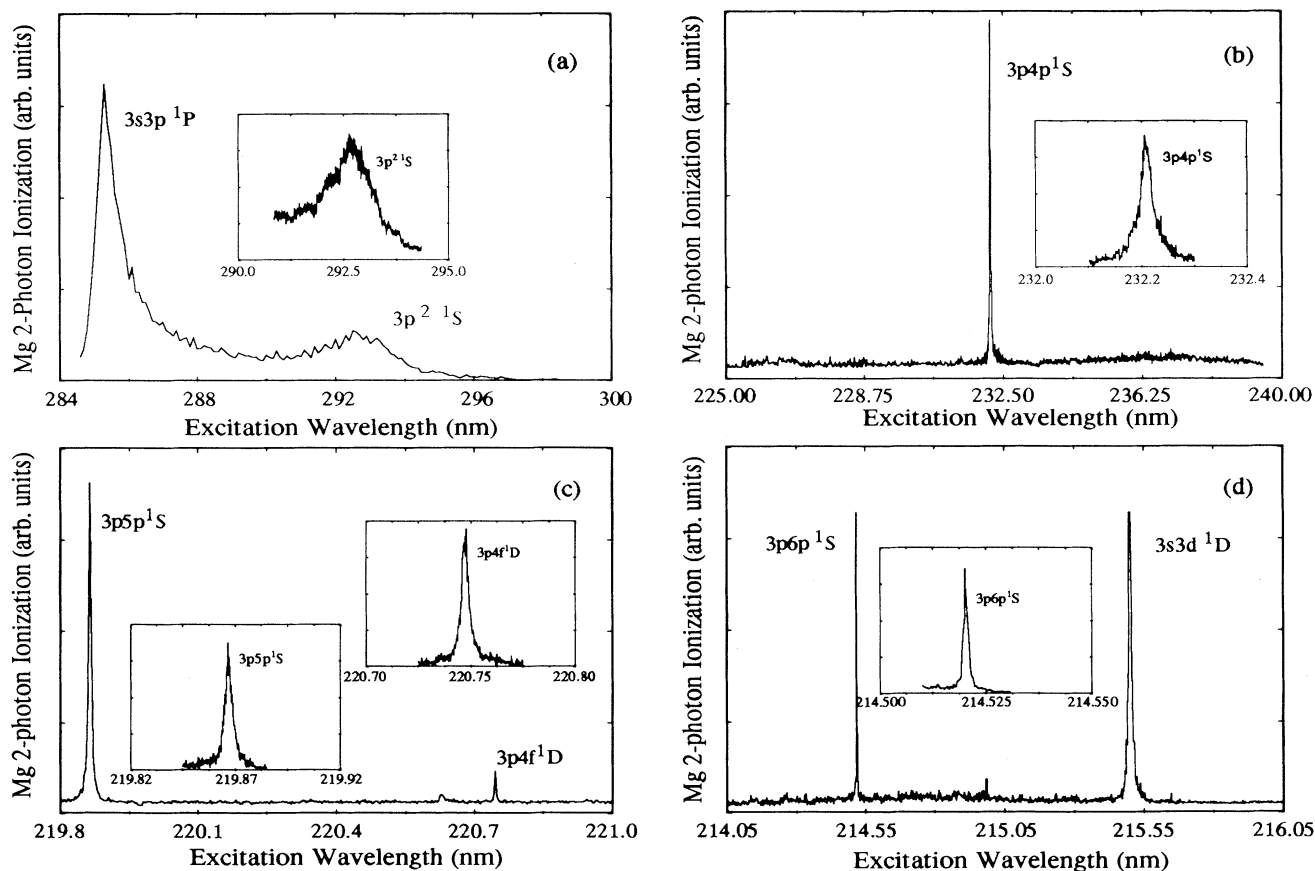


FIG. 2. Two-photon ionization spectra of Mg via the $3s3p\ ^1P$ and $3p^2\ ^1S$ (a); the $3p4p\ ^1S$ (b); the $3p5p\ ^1S$ and $3p4f\ ^1D$ (c); and $3p6p\ ^1S$ and $3s3d\ ^1D$ (d). The inserted spectra depict high-resolution runs around the state under investigation. Wavelength is vacuum corrected.

Ref. [10]. The peaks at vacuum wavelength of 285.30 nm [Fig. 2(a)] and 215.50 nm [Fig. 2(d)] correspond to the single-photon excitation of the $3p^1P$ and $3d^1D$ states, the latter via a quadrupole transition. All other peaks of the spectra originate from the two-photon autoionization of the doubly excited $3pnp^1S$ ($n=3-6$) series and the $3p4f^1D$ state. The broad peak at 293 nm can be attributed to the $3p^2S$ state as measured by Bonanno, Clark, and Lucatorto [5]. Its pronounced width, in comparison to all other observed peaks, is obviously due to the strong correlation of the two equivalent $3p$ electrons. In a classical picture, the overlapping of such orbits is further increased for the present minimum total orbital angular momentum of these two p electrons, which requires more or less the two orbits of the electrons to coincide. The assignment of the other autoionization peaks, observed in this work, is based on the comparison with the calculated spectra of Chang and Tang [8]. The agreement of the measured to the calculated spectra is fairly good. This allows the assignment of the peaks at 232.21, 219.86, 214.52, and 220.75 nm as originating from the decay of the two-photon excited $3p4p$, $3p5p$, $3p6p^1S$, and the $3p4f^1D$ states. A verification of the total angular momentum of the observed states has been done by recording the same spectral region using circularly polarized light. As can be seen in Fig. 3, only the $3p4f^1D$ ($J=2$) peak remains in the spectrum, as expect-

ed for the two-photon excitation, having slightly higher intensity than in the spectrum taken with linear polarization. It has been shown for the alkaline-earth elements that circular polarization may lead to larger multiphoton ionization (MPI) rates [11]. This can be attributed to the possibly larger transition probabilities when coupling different M_J levels. For example, the transition $|J, M_J=J\rangle \rightarrow |(J+1), M_J=J+1\rangle$ has larger probability than the transition $|J, 0\rangle \rightarrow |(J+1), 0\rangle$, except for $J=0$.

A comparison of the measured peak positions and the results of the calculations of Chang [7], Chang and Tang [8], and Moccia and Spizzo [9] are summarized in Table I. The measured autoionizing resonance positions are found to the blue side of all three calculations. However, the best agreement between experiment and theory is found with the recent results of Chang and Tang [8] with a largest shift of 210 cm^{-1} for the $3p4f^1D$ state.

The widths of the measured autoionizing states can be better seen in the high-resolution spectra inserted in Figs. 2(a)–2(d). In order to exclude any laser power broadening of the lines, a laser-intensity dependence of the width has been performed. The widths given in Table I correspond to laser intensities at which they have been stabilized to their minimum value. Their dependence on the quantum numbers n and l is as qualitatively expected. For the $3pnp^1S$ series, it decreases with increasing number n , due to the weaker electron-electron Coulombic in-

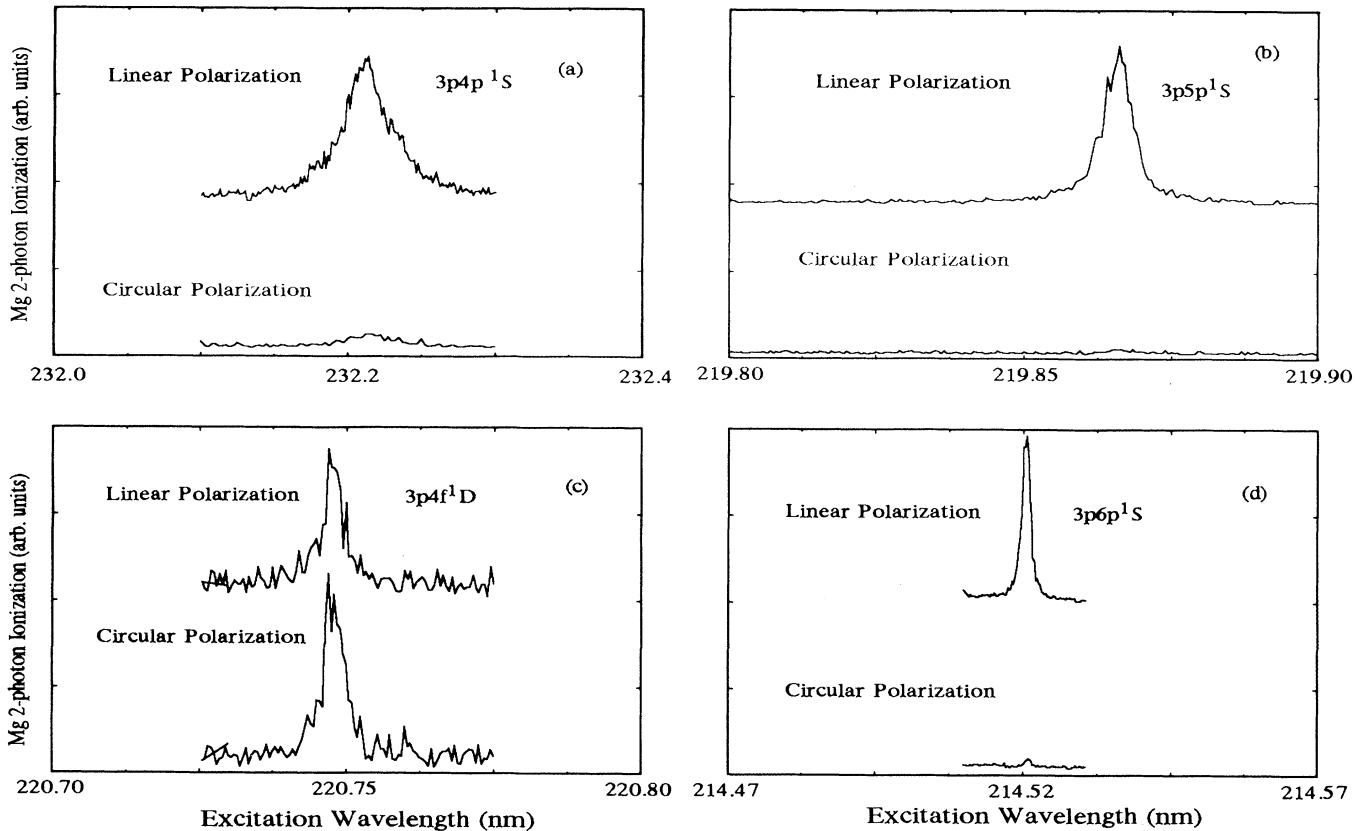


FIG. 3. Autoionizing states (a) $3p4p^1S$, (b) $3p5p^1S$, (c) $3p4f^1D$, and (d) $3p6p^1S$ excited by linearly and circularly polarized light. Wavelength is vacuum corrected.

teraction, as a consequence of the decreasing overlap of their orbitals. The decrease is more rapid than the $1/n^3$ scaling law [12] since we are not dealing with high Rydberg states. The much smaller observed width of the $3p4f^1D$ than that of the $3p4p^1S$ state can be understood in a simple classical picture as being due to the larger eccentricity of the elliptical orbit corresponding to the $4p$ electron and hence to its smaller perihelion distance [12]. Moreover the tendency for the widths, i.e., the dependence on n and l , of these autoionizing states is consistent with the calculated results of Chang and Tang [8], and Moccia and Spizzo [9] (see Table I). A very good agreement between the measured and calculated ionization profile [8] has been found for the $3p4p^1S$ state. However, the widths for autoionizing states lying energetically higher are in less good agreement with the theoretical ones. In general, they are found larger than the calculated widths (see Table I).

The spectra of Figs. 2(a)–2(d) are not recorded with the same laser intensity so that no relative intensities for all the observed peaks can be extracted from them. However, the dominance of the peak corresponding to the $3p^2^1S$ state is unambiguous since this peak could be easily observed with an unfocused laser beam corresponding to a power density of $\sim 10^6$ W/cm² while for the observation of the $3pnp^1S$ ($n > 3$) series power densities of the order of $\sim 10^8$ W/cm² had to be employed through focused laser beams. This profound dominance, which is due to (a) the two strongly correlated $3p$ electrons and (b) the near-resonant $3s3p^1P$ intermediate state, is also found in the calculated spectra [8], in which the ionization cross section ratio of the $3p^2^1S$ states to other states is about 10^2 . Moreover the peak height corresponding to the $3p4f^1D$ state is measured to be smaller than that of the $3p5p^1S$ state, as can be seen in Fig. 2(c). The intensity comparison could be done here because the laser power density was about the same in the excitation of both states. The observed relative amplitudes of these two peaks are consistent with those of the calculation of Chang and Tang [8]. The low intensity of the $3p4f^1D$ peak might be qualitatively attributed to the forbidden two-photon excitation of the $nfnf$ configuration from the ground state $3s^2^1S$, although the transition to the $3p4f^1D$ state is parity and total-angular-momentum allowed. The excitation of the state is due to the nonpure

character of it and the ground state. Thus the 6.5% $3p^2$ configuration admixture of the ground state, given by the multiconfigurational calculation of Kotochigova [13], and probable $3pnp$ admixtures in the 1D state might be the main contributions to the two-photon transition probability.

In contrast to the heavier alkaline-earth atoms Sr, Ba, and even Ca, no triplet states have been observed in the present studies. This is compatible with the purer LS coupling of the lighter element Mg, which excludes singlet-triplet mixing. Furthermore, in very good agreement with the theoretical calculations [8,14], no peaks corresponding to $3pnp^1D$ states have been observed. In addition, the absence of peaks originating from the decay of the $3p5f^1D$ and $3p7p^1S$ states expected to be observed at about 215.49 and 212.18 nm [8], respectively, is due to the low conversion efficiency of the BBO crystal at these wavelengths and the small width of these states. The large peak observed at 215.50 nm will be discussed below.

The quadrupole excitation of the $3s3d^1D$ state

The peak observed at 215.50 nm is attributed to the single-photon ionization of the $3s3d^1D$ state which is resonantly excited via a quadrupole transition from the ground state. This has been verified in several different ways. MPI spectra taken with the fundamental and the second harmonic of the laser beam have shown a peak at 431.00 and 215.50 nm, respectively. The exact coincidence of the peak positions in these spectra is already convincing enough that this peak is due to the $3s3d^1D$ state reached by two-photon dipole absorption or single SH photon quadrupole absorption, respectively, since no other known state can be assigned to it in both spectra. In recording these spectra, the laser intensity was kept as low as necessary so as to ensure no observable ac Stark shift. This excludes the possibility that the coincidence in the position of the two peaks is due to such a shift.

A verification of the single-photon excitation of the $3s3d^1D$ state via quadrupole transition has also been done via photoelectron spectroscopy using two copropagating laser beams temporally delayed to each other by 12 ns, which is almost the laser pulse duration. The first beam was set at 215.50 nm so as to match the quadrupole

TABLE I. Positions (E_0) and widths ($\Gamma_{1/2}$) of the autoionizing states. (a) The experimental result of this work, (b) Chang and Tang [8] [L^2 configuration-interaction (CI) calculation], (c) Chang [7] (Fano-configuration-interaction calculation), (d) Moccia and Spizzo [9] (L^2 CI calculation).

	Experimental (a)		Calculation (b)		Calculation (c)		Calculation (d)	
	E_0 (cm ⁻¹)	$\Gamma_{1/2}$ (cm ⁻¹)	E_0 (cm ⁻¹)	$\Gamma_{1/2}$ (cm ⁻¹)	E_0 (cm ⁻¹)	$\Gamma_{1/2}$ (cm ⁻¹)	E_0 (cm ⁻¹)	$\Gamma_{1/2}$ (cm ⁻¹)
$3p^2^1S$	68 273	280	68 200	314	68 130	271	67 936 ^a	331
$3p4p^1S$	86 129	7.0	85 985	6.58	85 423	0.59	85 362 ^a	6.78
$3p5p^1S$	90 964	1.7	90 777	0.521	90 175	4.3	90 125 ^a	0.46
$3p6p^1S$	93 231	0.6	93 023	0.0214	92 400	4.5	92 364 ^a	0.055
$3p4f^1D$	90 601	1.6	90 391				89 796 ^a	0.24

^aThese values result from the difference of the photoelectron kinetic energy resulting from the decay of the autoionizing states and the ground-state energy related to the $3s$ threshold, as given by the authors [9].

excitation. The second delayed one, set at 500 nm, was used just to single-photon ionize the $3s3d^1D$ state. Both laser intensities have been kept low (10^5 and 10^6 W/cm², respectively) in order not to cause observable ionization when only one of the two beams was introduced [Figs. 4(a) and 4(b)]. Upon introduction of both beams, a photoelectron peak has been observed at 0.6 eV [Fig. 4(c)] which corresponds to an absorption of one photon from each beam. The fact that absorption from the second beam occurs 12 ns later ensures that the first photon excites a real state, the $3s3d^1D$ state. It further shows that after 12 ns there is still enough population in the $3s3d^1D$ state to give rise to observable ionization, which is consistent with the 80-ns lifetime of this state [15]. The peak at 0.2 eV in Figs. 4(a) and 4(c) is due to photoelectrons originating from the walls of the vacuum chamber due to the scattered uv light, and hence does not show any resonant behavior as the wavelength is tuned.

A similar result has been obtained in MPI spectra taken with the fundamental and SH together, temporally overlapping. By keeping the two intensities very low, so that ionization due to one of the beams is just observable, a strong enhancement of the ionization peak has been observed when both beams were introduced. This enhancement is much stronger than the ionization intensity resulting from the summation of the ionization signals of

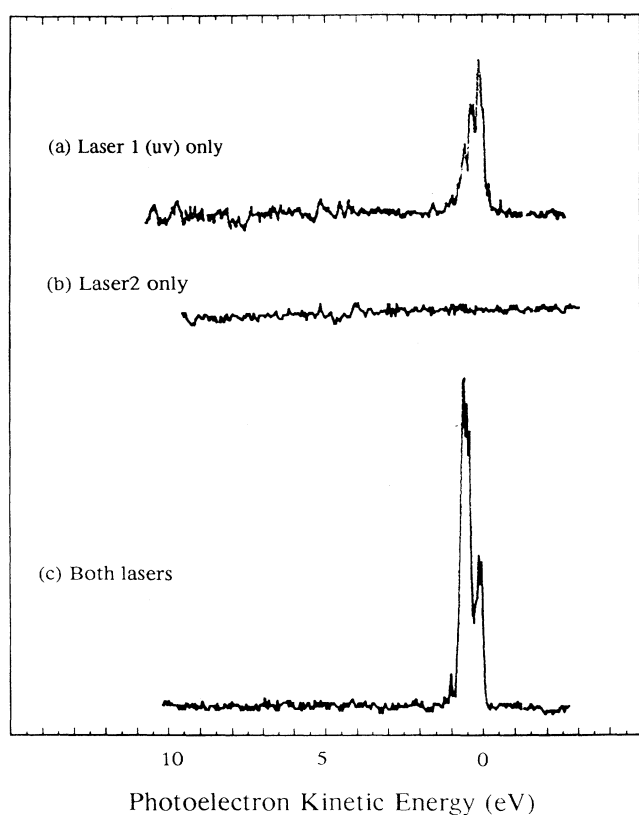


FIG. 4. Photoelectron kinetic-energy spectra resulting from (a) laser 1 (uv) only; (b) laser 2 only; and (c) both lasers, where laser 2 is temporally delayed for about 12 ns with respect to laser 1 (see text for detail).

the two independent laser beams as depicted in Fig. 5. Combined with the photoelectron results of the two delayed beams discussed above, this enhancement is very likely to be because the path to the continuum, which includes single-photon quadrupole excitation of the $3s3d^1D$ state and its ionization via single-photon absorption of the fundamental frequency, is the stronger one compared to all other possible paths. Summarizing, the ionization peak of Mg at 215.50 nm is due to excitation of the $3s3d^1D$ state via single-photon quadrupole transition, this stating that electric-quadrupole transitions may contribute to MPI spectra even more strongly than higher-order dipole transitions.

Photoelectron angular distribution

For a more complete spectroscopic study, photoelectron angular distributions (PEAD) have also been recorded for some resonant states. PEAD's are well known to be a sensitive spectroscopic tool, since, when combined with theoretical calculations, they give additional information to that obtained from the MPI spectra, concerning phase shifts of the partial waves describing the outgoing electron and relative strengths of the different interfering ionization channels [16]. All measured angular distributions are shown in Figs. 6 and 7. The experimental PEAD's have been fitted to the well-known expression for an N -photon process given by

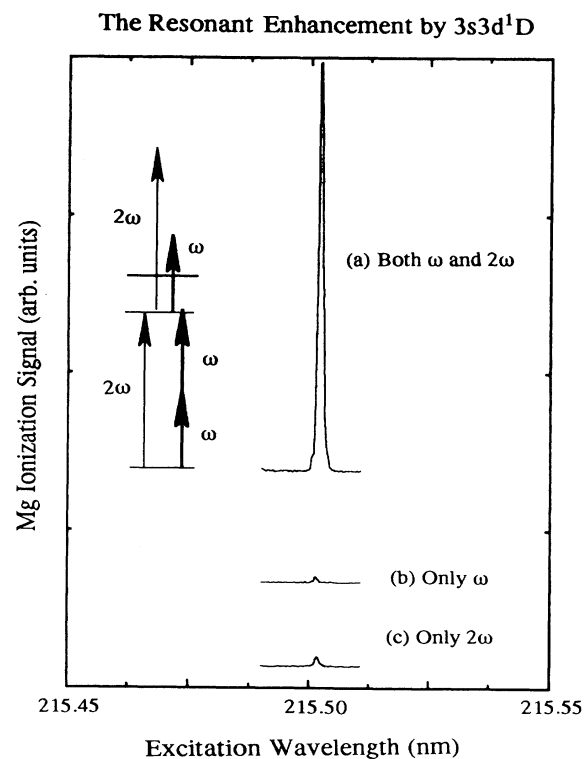


FIG. 5. The ionization enhancement resulting from (a) both quadrupole and dipole transitions; (b) the dipole transition only; and (c) the quadrupole transition only (see text for detail). Wavelength is vacuum corrected.

$$I(\theta) = \sum_{j=0}^N b_{2j} P_{2j}(\cos\theta) = \sum_{j=0}^N \beta_{2j} \cos^{2j}\theta, \quad (1)$$

where $P_{2j}(\cos\theta)$ is the Legendre polynomial of order $2j$, θ is the angle between the electric-field vector and the momentum of the photoelectron, and b_{2j} or β_{2j} are called asymmetry parameters determined by the atomic parameters. The resulting fitting asymmetry parameters β_{2j} for different states are summarized in Table II. The points in Figs. 6 and 7 represent the experimental data, the solid curves are least-squares fits to Eq. (1), while the dashed lines [in Figs. 6(a) and 6(b)] are results of the calculation of Tang [8].

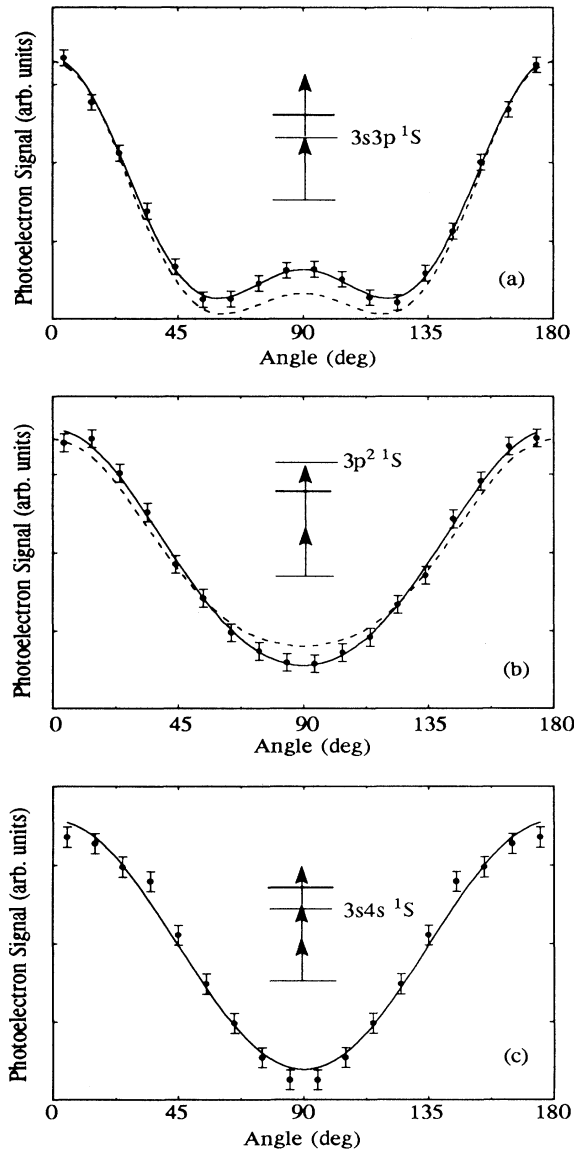


FIG. 6. PEAD resulting from 1+1 ionization via the $3s3p\ ^1P$ (a), $3p^2\ ^1S$ (b), and 2+1 ionization through the $3s4s\ ^1S$ (c) intermediate resonances. The solid line is the fit to Eq. (1), the dashed line in (a) and (b) is the theoretical calculation of Tang [8], and the quoted error bars are the standard deviation of the experimental data.

In the one-photon resonant two-photon ionization via the $3s3p\ ^1P$ state the PEAD [Fig. 6(a)] is very much like an $l=2$ Legendre polynomial (two minima at $\sim 55^\circ$ and $\sim 125^\circ$ and maxima at 0° and 90°). This indicates that from the two possible s and d partial waves, the d wave has the dominant contribution. Similar results have been obtained for the two-photon resonant three-photon ionization via the $3s3d\ ^1D$ [Fig. 7(a)] and $3s4s\ ^1S$ [Fig. 6(c)] states. In the case of the 1D resonance, from the two allowed p and f partial waves, the f (maxima at 0° , $\sim 64^\circ$, and $\sim 116^\circ$ and minima at $\sim 40^\circ$, 90° , and $\sim 140^\circ$) strongly dominates, as can be seen in Fig. 7(a). For the $3s4s\ ^1S$ state the angular distribution has an expected $\cos^2\theta$ dependence, characteristic for the p wave which is the only allowed one. Thus for all these three states the observed behavior is the expected one [17,18]. In the ionization step the channel which increases the angular momentum ($\Delta l = 1$) is the dominant one while the partial wave resulting from $\Delta l = -1$ can be considered as being negligible. Any attempt to measure angular distributions of electrons originating from the autoionization decay of the doubly excited $3pnp\ ^1S$ ($n > 3$) states has resulted in flat distributions. This isotropic emission is consistent with the $\Delta J = \Delta L = \Delta S = 0$ selection rule of autoionization via Coulombic interaction and it also confirms the $J=0$ assignment of the states. In contrast, the angular distribution of the decay of the $3p^2\ ^1S$ state in Fig. 6(b) is

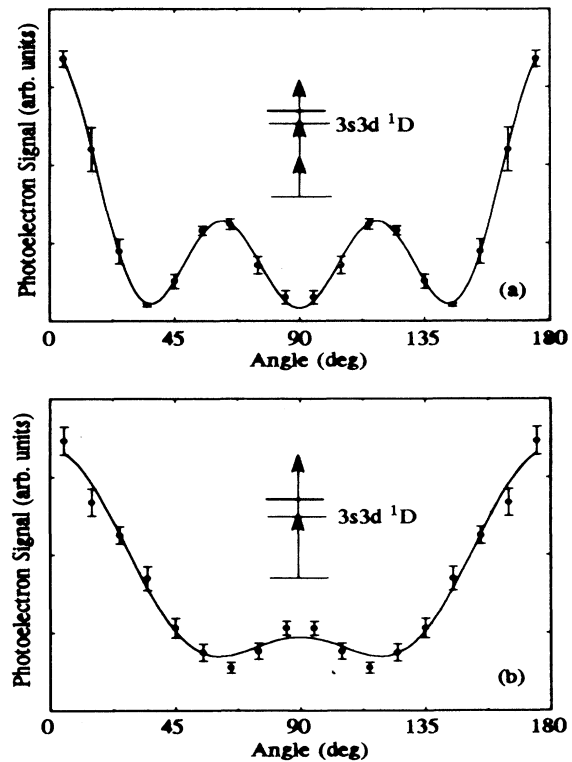


FIG. 7. PEAD resulting from 2+1 ionization via the $3s3d\ ^1D$ intermediate resonance (a), and 1+1 ionization via the $3s^2\ ^1S \rightarrow 3s3d\ ^1D$ quadrupole transition (b). The solid line is the fit to Eq. (1) and the quoted error bars are the standard deviation of the experimental data.

TABLE II. Fitting parameters of Eq. (1) to the PEAD resulting from 1+1 ionization via the $3s3p\ ^1P$ intermediate resonance; two-photon ionization via the $3p^2\ ^1S$ autoionizing state; 2+1 ionization via the $3s3d\ ^1D$ intermediate resonance; 1+1 ionization via the $3s3d\ ^1D$ state through the quadrupole transition; 2+1 ionization via the $3s4s\ ^1S$ intermediate resonance. β_0 has been normalized to unity and the error associated with it is zero.

β_{2i}	β_0	β_2	β_4	β_6
$3s3p\ ^1P(1+1)$	1	-4.51 ± 0.43	8.74 ± 0.60	
$3p^2\ ^1S$ two-photon	1	4.08 ± 0.63	1.39 ± 0.44	
$3s3d\ ^1D(2+1)$	1	69.86 ± 12.8	212.87 ± 37.98	163.37 ± 28.68
$3s3d\ ^1D(1+1)$	1	-2.24 ± 0.30	2.81 ± 0.35	
$3s4s\ ^1S(2+1)$	1	15.41 ± 1.0		

not isotropic. This PEAD has been recorded at a laser wavelength corresponding to the maximum of the autoionizing resonance. This anisotropy implies that the d -wave contribution to this two-photon ionization is not negligible compared with that of the s wave. The calculated PEAD's of Tang [8] for the $3s3p\ ^1P$ and $3p^2\ ^1S$ states are in very good agreement with our experimental results [see Figs. 6(a) and 6(b)].

Finally the PEAD, when ionization is via quadrupole excitation of the $3s3d\ ^1D$ state, as can be seen in Fig. 7(b), is quite different than that when the excitation is via dipole interaction [Fig. 7(a)]. Besides the different alignment that the two excitation schemes produce in the intermediate state, the PEAD in the case of the quadrupole transition has also an azimuthal angle ϕ dependence. Interference is now not only between the partial waves in θ but also in ϕ [19]. Thus the simple considerations as made above for the dipole transitions do not apply here. The summations $\sum_j \beta_{2j} \cos^{2j}\theta$ describing the PEAD at $\phi = \pi/2$, as is the case in the present experiment, will not include $j = 3$ as in the case of dipole transition since the term with $j = 3$ vanishes due to the interference of partial waves in ϕ [19].

SUMMARY

We have presented the spectroscopy of Mg autoionizing states $3pnp\ ^1S$ ($n = 3-6$) and $3p4f\ ^1D$ obtained via direct two-photon excitation with laser wavelengths covering the 300–214-nm region. The measured positions, and the excitation magnitude of those autoionizing states,

are in partial agreement with the *ab initio* calculations. A very good agreement has been found for the ionization profile of the $3p4p\ ^1S$ state; however, there are discrepancies for the widths of the autoionizing states lying energetically higher. Both linearly and circularly polarized light have been used in order to verify the assignment of total angular momentum.

A strong single-photon quadrupole transition $3s^2\ ^1S - 3s3d\ ^1D$ has been observed and reported. This transition might provide an alternative scheme for phase-controlled measurements of ionization or PEAD [20], in which the excitation of the 1D state is through the single-photon (quadrupole transition) and two-photon (dipole transition) interfering channels, by changing the relative phases of the fundamental and second-harmonic radiation.

Photoelectron angular distributions have been measured for several cases. A comparison with theoretical calculation has been made for the PEAD resulting from 1+1 ionization via $3s3p\ ^1P$ intermediate resonance and two-photon ionization via $3p^2\ ^1S$ autoionizing state with good agreement found.

ACKNOWLEDGMENT

This work has been carried out in the Ultraviolet Laser Facility operating in the Institute of Electronic Structure and Laser of the Foundation for Research and Technology–Hellas with support from the Large Installations Plan (Project No. G/89100086/GEP) of the European Community (DG XII).

- [1] D. Kim, S. Fourier, M. Saeed, and L. F. DiMauro, Phys. Rev. A **41**, 4966 (1990); M. Y. Hou, P. Breger, G. Petite, and P. Agostini, J. Phys. B **23**, L583 (1990).
- [2] S. E. Harris, Phys. Rev. Lett. **62**, 1033 (1989).
- [3] C. J. Dai, S. M. Jaffe, and T. F. Gallagher, J. Opt. Soc. Am. B **6**, 1486 (1989); M. Kompitsas, S. Goutis, M. Aymar, and P. Camus, J. Phys. B **24**, 1557 (1991); V. Lange, U. Eichmann, and W. Sandner, *ibid.* **22**, L245 (1989); C. J. Dai, G. W. Schinn, and T. F. Gallagher, Phys. Rev. A **42**, 223 (1990); S. Goutis, M. Aymar, M. Kompitsas, and P. Camus, J. Phys. B **25**, 3433 (1992).
- [4] J. O. Gaardated, T. Andersen, H. K. Haugen, J. E. Hansen, and N. Vaeck, J. Phys. B **24**, 4363 (1991).
- [5] R. E. Bonanno, C. W. Clark, and T. B. Lucatorto, Phys. Rev. A **34**, 2082 (1986).
- [6] M. D. Lindsay, L. T. Cai, G. W. Schinn, C. J. Dai, and T. F. Gallagher, Phys. Rev. A **45**, 231 (1992); G. W. Schinn, C. J. Dai, and T. F. Gallagher, *ibid.* **43**, 2316 (1991).
- [7] T. N. Chang, Phys. Rev. A **36**, 5468 (1987).
- [8] T. N. Chang and X. Tang, Phys. Rev. A **46**, 2209 (1992); X. Tang (private communication).
- [9] R. Moccia and P. Spizzo, J. Phys. B **21**, 1121 (1988).
- [10] V. Kaufman and W. C. Martin, J. Phys. Chem. Ref. Data **20**, 83 (1991).
- [11] P. Lambropoulos, Phys. Rev. Lett. **28**, 585 (1972).
- [12] T. F. Gallagher, W. E. Cooke, and K. A. Safinya, in *Laser*

- Spectroscopy, Proceedings of the 4th International Conference*, edited by H. Walther and K. W. Rothe (Springer, Berlin, 1979), p. 273.
- [13] S. A. Kotochigova (private communication).
- [14] R. Moccia and P. Spizzo, *J. Phys. B* **21**, 1145 (1988).
- [15] G. Jonsson, S. Kroll, A. Persson, and S. Svanberg, *Phys. Rev. A* **30**, 2429 (1984).
- [16] X. Tang, T. N. Chang, P. Lambropoulos, S. Fourier, and L. F. DiMauro, *Phys. Rev. A* **41**, 5265 (1990).
- [17] G. Leuchs and H. Walther, in *Multiphoton Ionization of Atoms*, edited by S. L. Chin and P. Lambropoulos (Academic, Toronto, 1984), p. 109.
- [18] H. Rottke, B. Wolff, M. Brickwedde, D. Feldmann, and K. H. Welge, *Phys. Rev. Lett.* **64**, 404 (1990).
- [19] A. Lyras, B. N. Dai, X. Tang, P. Lambropoulos, Adila Dodhy, J. A. D. Stockdale, Dino Zai, and R. N. Compton, *Phys. Rev. A* **37**, 403 (1988).
- [20] Ce Chen, Yi-Yian Yin, and D. S. Elliott, *Phys. Rev. Lett.* **64**, 507 (1990); Yi-Yian Yin, Ce Chen, D. S. Elliott, and A. V. Smith, *ibid.* **69**, 2353 (1992); Shao-Ping Lu, Seung Min Park, Yongjin Xie, and Robert J. Gordon, *J. Chem. Phys.* **96**, 6613 (1992).